APAS-TR

Automatic **P**PP **A**nalysis **S**oftware-Türkiye

User Manual

(Version 1.0)

Sinan Birinci & Mehmet Halis Saka

e-mail: s.birinci@gtu.edu.tr

Gebze Technical University
Kocaeli, Türkiye

May 2024

Contents

1. Overview

The Precise Point Positioning (PPP) approach can meet the need for millimeter-to-centimeter accuracy with a single receiver, removing the requirement for an external GNSS receiver. Initially, PPP applications were limited to utilizing observations from GPS satellites. However, over the decade, the successful launch of GLONASS, Galileo, and BDS has made worldwide multi-GNSS PPP options possible. In other words, when the PPP applications are applied with the integration of four global constellations, a significant enhancement is realized in both the number of satellites and satellite geometry. Thus, the multi-GNSS combinations help speed up the convergence in PPP by allowing the estimated parameters to reach their real values more quickly, which is a significant drawback of the PPP method. The multi-GNSS PPP not only reduces convergence time but also increases positioning accuracy and precision. Nevertheless, in both the functional and stochastic models, the processing procedure for different constellations is considerably more sophisticated and detailed than that of a single system.

Automatic **P**PP **A**nalysis **S**oftware-Türkiye (APAS-TR) is a MATLAB-based open-source multi-GNSS software package written by Sinan Birinci. The software provides traditional PPP solutions that the ambiguity is as a float by generating ionosphere-free linear combinations of dual-frequency code and phase observations. The main features of APAS-TR are as follows.

- Multi-GNSS PPP processing with GPS, GLONASS, Galileo, BDS-2, BDS-3, and QZSS satellites (The navigation satellite system frequencies available to the software are listed in Table 1.)

Table 1. List of frequencies used in the APAS-TR software.

Satellite System	First Frequency	Second Frequency
GPS	L1	L2
GLONASS	G1	G2
Galileo	E1	E5a
BDS-2	B1	B3
BDS-3	B1	B3
QZSS	L1	L2

- Receiver clock jump detection and repairing
- Smoothing code measurements with phase measurements

- Cycle Slip detection and repairing: Rate of total electron content index (ROTI)-based geometry-free combination, the forward and backward moving window averaging (FBMWA) for the Melbourne–Wübbena combination.
- Abundant tropospheric modeling options
- Weighting models based on satellite elevation angle and carrier-to-noise-density ratio (C/N0)
- Setting the standard deviations of code and phase measurements for all satellite system
- The Median Absolute Deviation (MAD) based approach to detecting outliers.
- Computing statistical results of outputs and extensive plotting options

2. Requirements and Installation

The APAS-TR software has been developed and tested using the MATLAB platform under the Windows operating system. A current MATLAB version is required to use the software. To access the software interface, open the APAS_TR folder in your current MATLAB working directory. Then, start the software interface by running the **execute_APAS_TR.m** code in this folder.

3. Software Structure

APAS-TR consists of 4 main menus. These are ***Inputs**, ***Models**, ***Filtering**, and ***Outputs** sections. Note that the software contains separate folders for the necessary inputs (observation file, satellite orbit and clock products, DCB, antenna, troposphere, and Sinex files). Therefore, the dataset and products should be placed in the appropriate folders. For example, when you want to import the satellite orbit file into the software, the software will first search in the APAS_TR\Inputs\Orbit_Products folder.

3.1. Inputs Menu

When the software is opened for the first time, the user is presented with the page shown in Figure 1. This page introduces the observation file necessary for beginning the PPP evaluation procedure in the software. The Rinex observation file can be uploaded to the program with the Rinex File button (1).

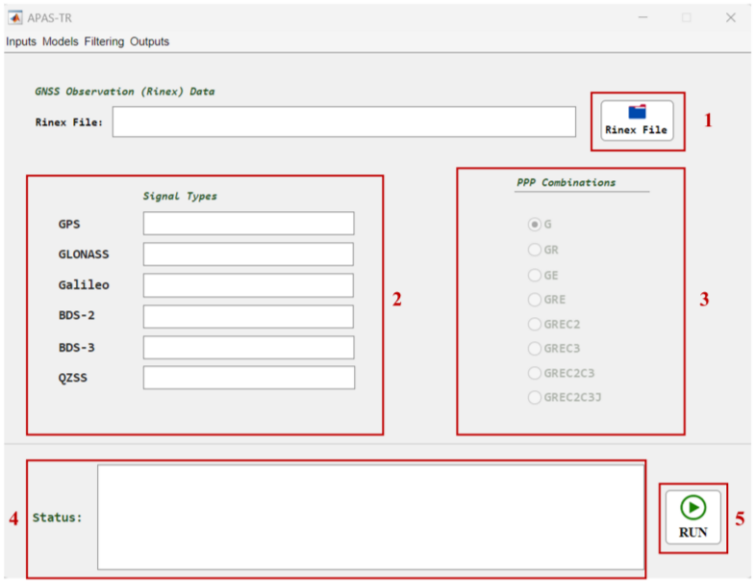

Figure 1. The first page after run-up APAS-TR (Inputs>Rinex Data)

The software reads the observation file of the GNSS station. The available satellite systems in the station data are highlighted in green, and the eight different GNSS combinations that can be utilized are enabled correspondingly (2 and 3). Additionally, the user is presented with the progress steps on the status panel after beginning software usage (4). After completing all the required inputs and changes, the PPP solution can be started by clicking the RUN button (5).

In the next step, the satellite orbit and clock products that are appropriate for the date range in which the station's data is should be supplied to the program. This is accomplished by opening the submenu under the heading Inputs>Orbit and Clock Products. The products can be loaded in the software using the Orbit File (1) and Clock File (2) buttons shown in Figure 2.

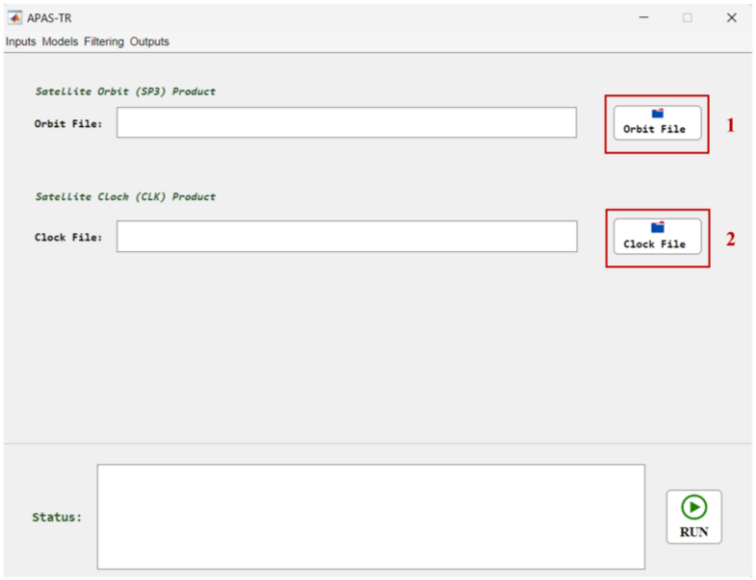

Figure 2. Input>Orbit and Clock Product Submenu

Standard Product 3 (SP3) defines the format for providing GNSS satellite orbit and clock information. Initially released by IGS, orbit and clock products in SP3 format are now freely available from several Analysis Centers (ACs). These files are provided to users at a specified sampling rate. The final products typically have a sampling rate of 5 minutes for the orbit and 30 seconds for the clock offset. The sampling interval of observation files, which is the recording interval of observations by a GNSS receiver, is typically 30 seconds or less (15 s, 5 s, 1 s). Therefore, an interpolation procedure is crucial for the orbit and clock products. This software utilizes ninth-order Lagrange interpolation for GNSS orbit interpolation and simple linear interpolation for clock offset interpolation.

The third step is to import the antenna and DCB (Differential Code Bias) files into the program. The DCB file is used to convert C/A-code measurements for GPS and GLONASS to P-code measurements and is optional. The antenna file is required to calibrate both the satellite and receiver antennas. This program page is also shown in Figure 3. The Antex File (1) and DCB File (2) buttons allow related files to be added to the program.

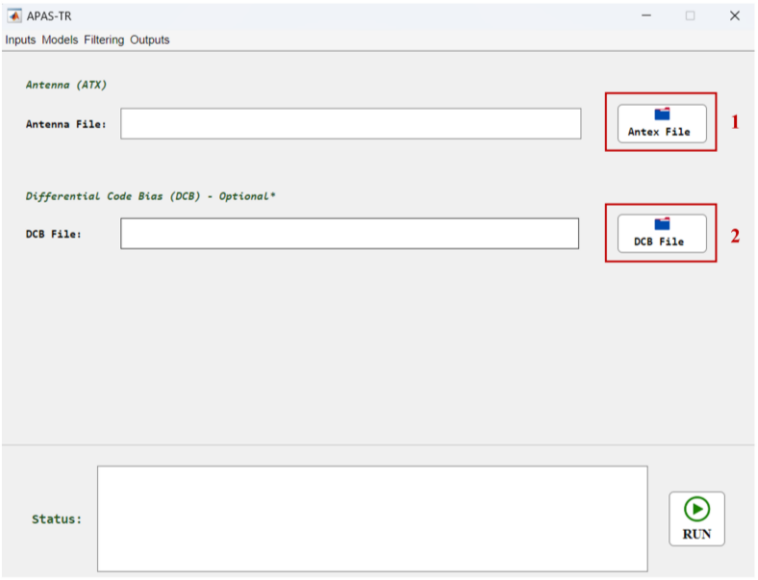

Figure 3. Inputs>Antenna and DCB Files Submenu

3.2. Models Menu

The Models Menu of the program comprises two submenus. The first component is the Satellite and Receiver Dependent section as seen in Figure 4.

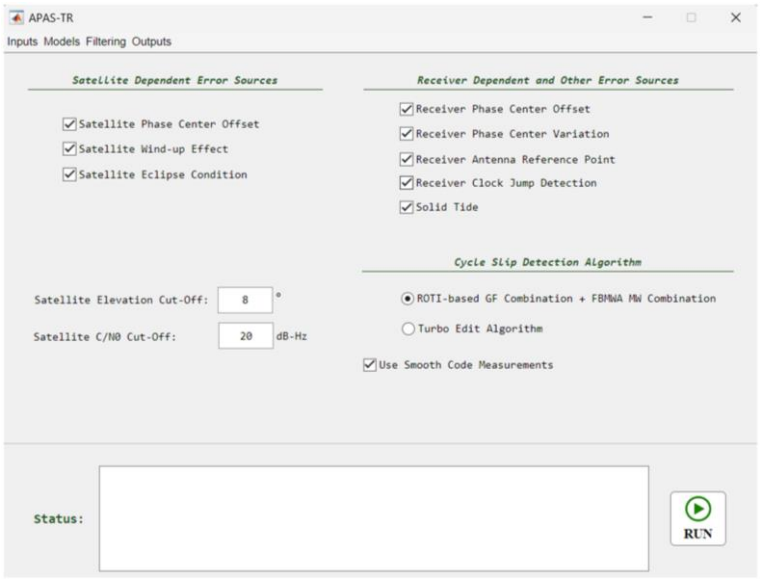

Figure 4. Models>Satellite and Receiver Dependent Submenu

This section contains check boxes used to include and ignore systematic errors associated with the satellite and the receiver in the model. There is also the option of smoothing code measurements with phase measurements. The satellite elevation angle and the carrier-to-noise ratio (C/N0) cut-off values can be set for different situations. The software presents a more reliable algorithm considering the ionospheric effect to avoid falsely detecting cycle slips during high ionospheric activity. In this algorithm, the threshold value of the geometry-free combination varies as a function of the rate of total electron content index (ROTI) (Luo et al. 2022). In addition, the forward and backward moving window averaging (FBMWA) technique was also used to detect small cycle slips by reducing the noise in the Melbourne-Wubbena combination (Cai et al. 2013). Besides this, users are also provided with the option to utilize the Turbo-Edit method, which is widely employed in several software (Blewitt 1990).

The Atmosphere is in the second submenu. Five distinct atmospheric correction models for the troposphere, one of the major error sources in the PPP, are offered to the user in this section (Figure 5).

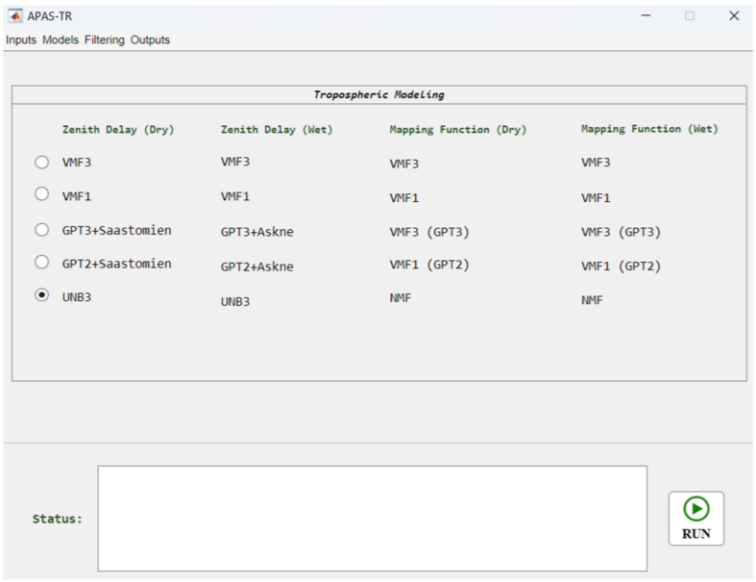

Figure 5. Models>Atmosphere Submenu

The troposphere is divided into four sections. These are the zenith dry delay, the zenith wet delay, and the mapping functions for these components. The software can use two different Vienna Mapping Function (VMF) versions. When a VMF version is selected and an Internet

connection is available, the associated auxiliary files are downloaded into the appropriate folder (Kouba 2008). In addition to the VMF1 (Boehm et al. 2006), and VMF3 models (Landskron and Böhm 2018), which use grid files, the Saastamoinen model (Saastamoinen 1972) for the dry section and the Askne-Nordius model (Askne and Nordius 1987) for the wet section can be applied. These models employ metrological data obtained from the Global Pressure and Temperature 3/2 (GPT 3/2) models (Böhm et al. 2015), (Landskron and Böhm 2018). Note that the models do not accurately estimate the wet component; it was only utilized as an a priori value in the functional model. Alternatively, the UNB3 empirical model developed by the University of New Brunswick can also be implemented (Leandro et al. 2006).

3.3. Filtering Menu

Previous parts addressed reading input files, pre-preparation, handling, and eliminating error sources. The Filtering section includes the Adjustment Setting submenu. The left part of the sub-menu consists of the standard deviations of the parameters that need to be estimated for the initial states and the system noise of these parameters. Furthermore, the a priori standard deviations of the code and phase observations can be changed, and different standard deviation values can be set for each satellite system. This menu also allows the user to select from three weighting models. These are to ensure that the Kalman filter performs successfully. A detailed view of this submenu can be seen in Figure 6.

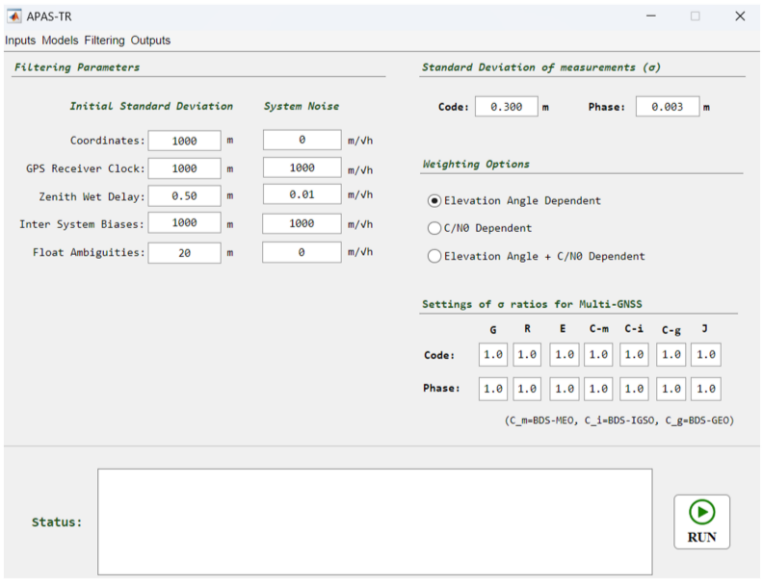

Figure 6. Filtering>Adjustment Settings Submenu

3.4. Outputs Menu

The Outputs section comprises two submenus. PPP solutions must be performed using the RUN button before proceeding to evaluate with the Analysis submenu (Figure 7).

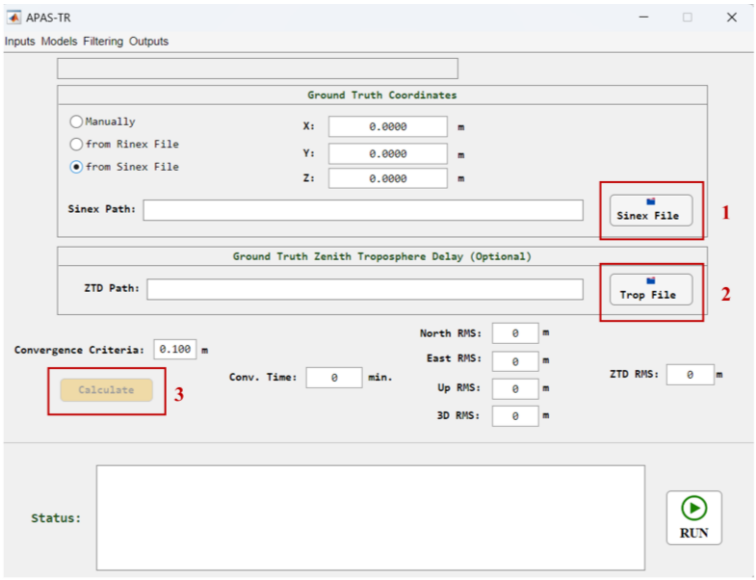

Figure 7. Outputs>Analysis Submenu

Once the solution has been completed, the ground truth coordinates of the station provide the fundamental input for the analysis. The software obtains the precise coordinates of the station by reading the Sinex file for IGS stations (by clicking the Sinex File button (1)). If the station is not an IGS station or not listed in the Sinex file, coordinates can be manually inserted into the program. Thus, users are provided with convergence time, north, east, up, and 3D RMS values based on the ground truth coordinates and convergence criteria using the Calculate button (3). Furthermore, the ZTD extension file is read (with Trop File button (2)); if the station's zenith tropospheric delay data is available, hourly precise ZTD values are obtained and compared with the PPP results. The RMS value of the tropospheric delay component from the PPP solution is also computed using the Calculate button (3).

The Plotting section is the second submenu of the Outputs menu. Visualization is essential for assessing and understanding different solutions. The software offers a wide range of advanced choices for plotting. Upon examining Figure 8 illustrates that ten plotting tools are available for

visualizing the software's results (1). Additionally, on the right side of the menu (2), residual values of code and phase measurements for each satellite system can also be plotted (by clicking the Plot button (3)). Moreover, it is also possible to plot the code and phase residuals for each satellite in each constellation with respect to the elevation angle and the first and second frequencies' C/N0 values (by clicking the Plot button (3)).

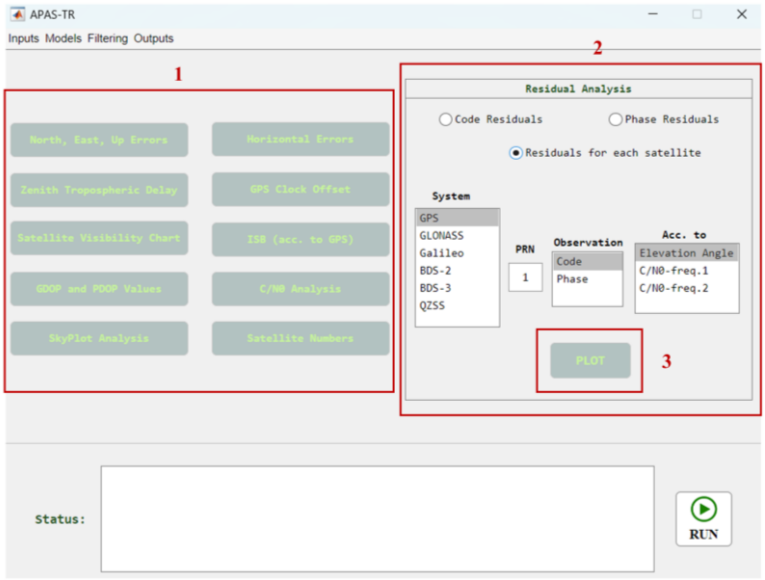

Figure 8. Outputs>Plotting Submenu

4. First PPP Processing

A PPP application was conducted for a selected GNSS station to facilitate the software's usability.

Table 2. Input files for the PPP processing procedure.

Rinex File	KARR00AUS_R_20233440000_01D_30S_MO.rnx
SP3 File	COD0MGXFIN_20233440000_01D_05M_ORB.SP3
Clock File	COD0MGXFIN_20233440000_01D_30S_CLK.CLK
Antenna File	igs20_2303.atx
DCB File (optional)	CAS0MGXRAP_20233440000_01D_01D_DCB.BSX
Sinex File	IGS0OPSSNX_20233440000_07D_07D_SOL.SNX
ZTD File	COD0OPSFIN_20233440000_01D_01H_TRO.TRO

Additionally, all outputs about the results and visualizations were presented in the last section. For this, the 24-hour observation dataset recorded at KARR station from the IGS MGEX network with a 30-second sampling interval on 10.12.2023 was employed. Table 2 contains all the files needed to execute the PPP processing and to analyze its performance.

4.1. Data Preparation

To perform the first PPP processing, the observation file must be stored in the ..\APAS_TR\Inputs\Rinex_Data directory.

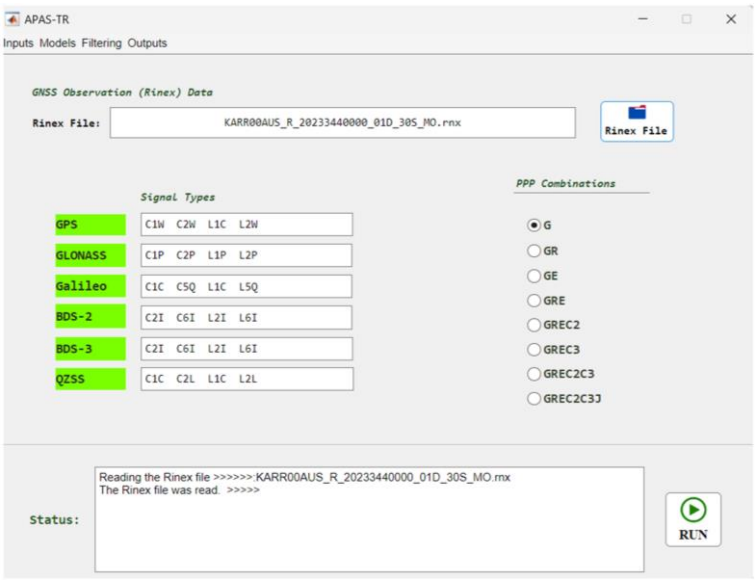

Figure 9. Importing the observation file into the software

The data preparation process starts by selecting the observation file. The file name appears in the Rinex File part after the file choice and read. According to the frequencies that the software can utilize and the available satellite systems, appropriate PPP combination options automatically become active. Besides, the steps taken can be inspected through the status panel.

The second step is to go to the Inputs>Orbit and Clock Products submenu and choose the satellite orbit and clock products that are appropriate for the date period for which the station's data is available. Figure 10 illustrates the layout of this page and the products being provided. After adding these products, the required updates will appear in the corresponding fields.

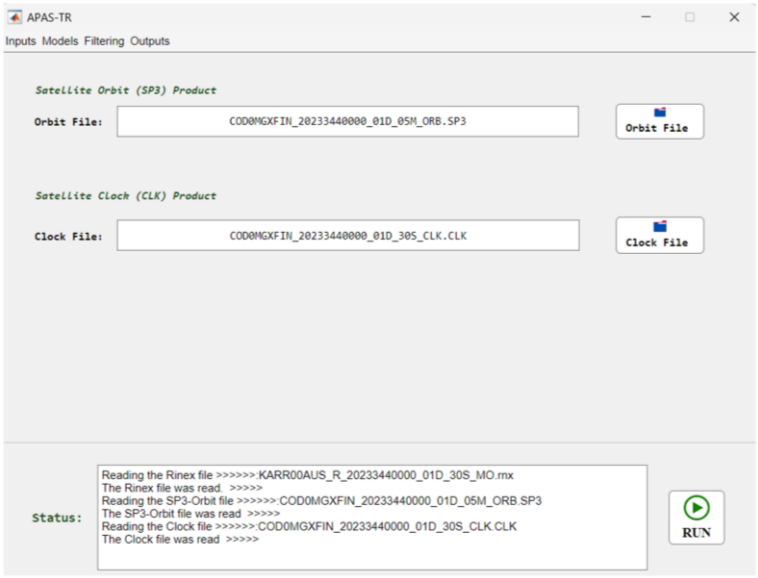

Figure 10. Importing the orbit and clock offset file into the software.

In the last step of data preparation, to ensure antenna calibration and convert C-code observations into P-code observations, go to the Inputs>Antenna and DCB Files submenu. The DCB file is optional, and the DCB values are used to pass to the P-code if the Rinex observation file contains the C-code for GPS and GLONASS code observations. Figure 11 depicts the addition of these files to the program and the subsequent changes in the status panel and other fields.

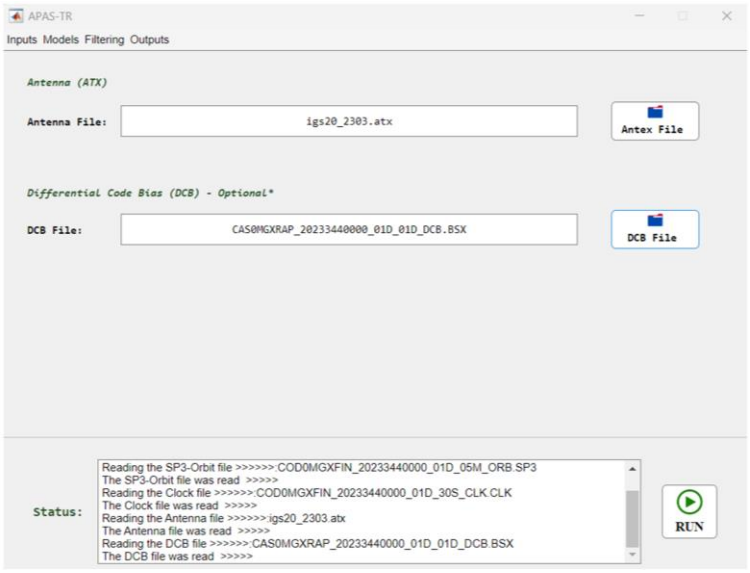

Figure 11. Importing the Antenna and DCB files into the software.

4.2. PPP Processing Strategies

Following the loading of necessary files into the program, high performance in the PPP evaluation technique relies on the quality of the functional and stochastic models. Potential error sources should be considered for PPP evaluation. If Figure 12 is examined, the Models>Satellite and Receiver Dependent submenu is presented, which contains options for not only the error sources related to the receiver and satellite but also for detecting and correcting cycle slip issues. The software also allows input of satellite elevation angle and C/N0 cut-off values.

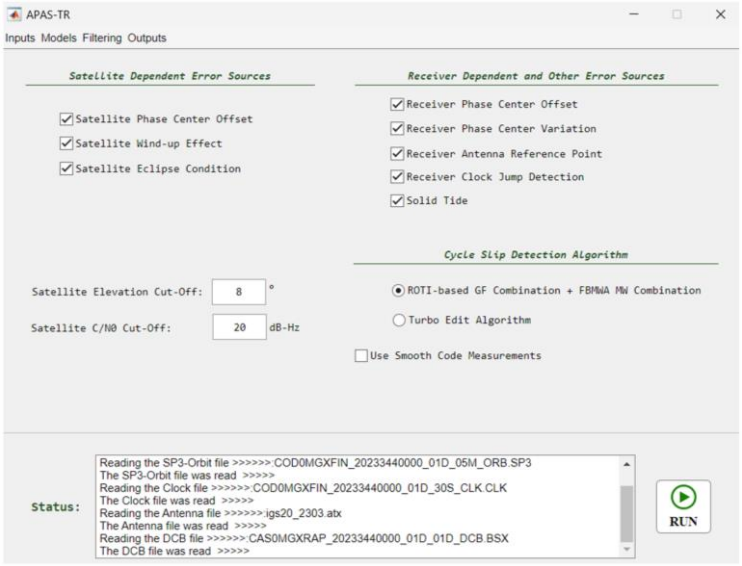

Figure 12. Error Sources Modeling and Cycle Slip Methods in APAS-TR Software

The APAS-TR software offers several models for the tropospheric delay, one of the most important sources of error in the PPP. Figure 13 shows the tropospheric model options in the Models>Atmosphere submenu. The VMF3 model was preferred for this application. It should be noted that the VMF3 and VMF1 models require an internet connection.

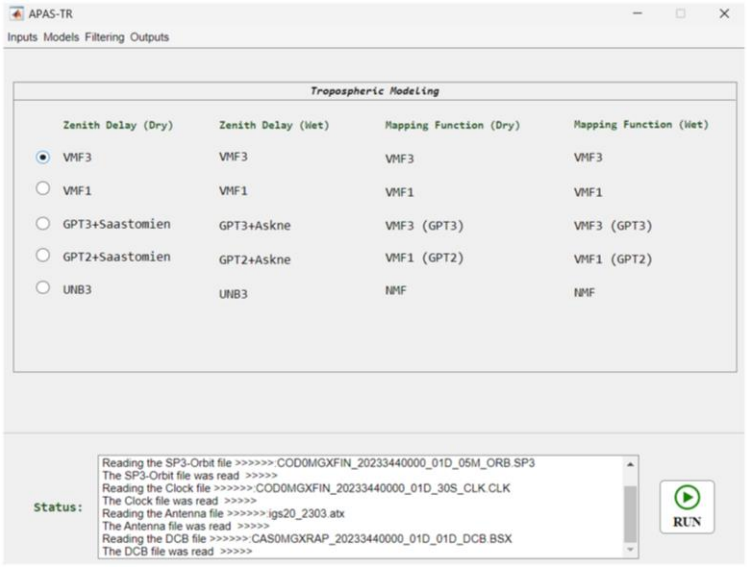

Figure 13. Tropospheric Delay Models

After implementing selections for the error sources in PPP, the user opens the Filtering>Adjustment Settings submenu to apply changes regarding the to-be-estimated parameters. For optimal performance of the Kalman Filter, users can modify the initial standard deviation values and system noises for unknown parameters, as illustrated in Figure 14. The values that are set by default are the ones that are consistent with the literature. If not modified, a static PPP solution will be executed. Meanwhile, applying changes to the system noise of the coordinate components is the first step that can be adopted to get kinematic solutions.

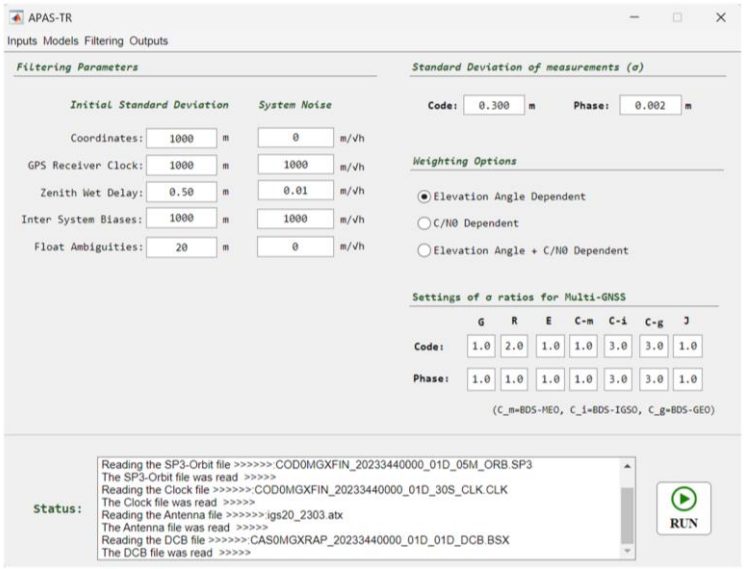

Figure 14. Adjustment settings for the stochastic modeling part of the Kalman Filtering

A-priori standard deviations can be determined for code and phase measurements. Furthermore, these values can be adjusted to each other for each navigation system. The weight of GLONASS code observations in the model should be decreased because of the Inter-Frequency Bias (IFB) term. The IGSO and GEO satellites of the BDS constellation should be given less weight compared to the MEO satellites due to the precision of their orbit and clock products. After all these standard deviation and ratio settings are made in Figure 14, the weight model should be selected according to the type of receiver and antenna. This study used a geodetic receiver and antenna and implemented weighting based on satellite elevation angle.

After completing all stages, PPP processing is started with the RUN button.

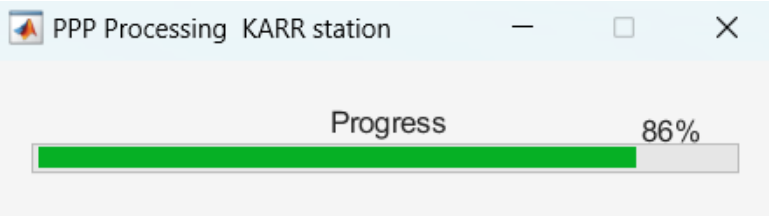

5. Analysis of Results and Plotting

5.1. Output file format description

At the end of the data evaluation process, the Outputs>Analysis submenu is automatically opened. A folder named after the station is created in the ..\APAS-TR\Results_File directory. In this folder, a sub-folder is created in the format day-month-year-hour-minute-second. The output file is saved as a txt extension in this folder. The output file is named PPP Combination-Station Name-results.txt. On June 10, 2024, the hierarchy of the folder where the output file of the KARR station, which was solved with the combination of GPS+GLONASS+Galileo+BDS2+BDS3+QZSS (GREC2C3J), is stored can be examined in Figure 15.

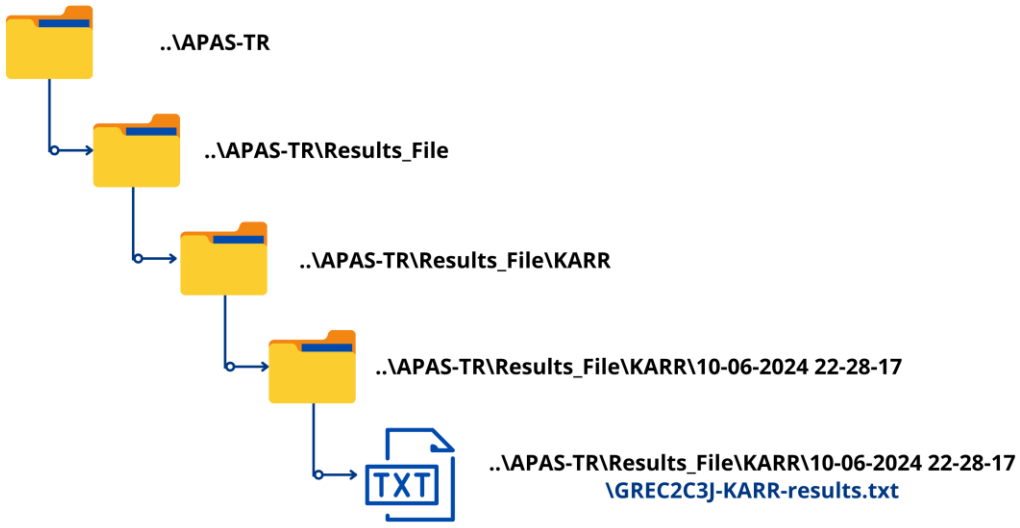

Figure 15. Path of the folder in which the output file of the KARR station is stored.

The content of the output file consists of time, receiver coordinates, GPS receiver clock offset, zenith tropospheric delay, and ISB values for GLONASS, Galileo, BDS-2, BDS-3, and QZSS satellite systems for each epoch, respectively. Figure 16 shows a part of the output file of the KARR station. Besides, the definitions of the formats of these parameters are provided in Table 2 for a more thorough examination.

Table 2. Format description for the output file of the APAS-TR software.

Column	Description	Unit	Value Type	Range
1	Epoch Number		int	1-5
2	Year	year	int	9-14
3	Day of Year	day	int	16-20
4	Second of GPS Week	second	int	25-39
5	X-coordinate	m	double	45-59
6	Y-coordinate	m	double	61-75
7	Z-coordinate	m	double	77-91
8	GPS receiver clock offset	m	double	92-108
9	Zenith Tropospheric Delay	m	double	109-122
10	ISB-GLONASS	m	double	123-136
11	ISB-Galileo	m	double	138-151
12	ISB-BDS-2	m	double	154-167
13	ISB-BDS-3	m	double	168-181
14	ISB-QZSS	m	double	183-196

GREC2C3J-KARR-results.txt

APAS-TR PPP Solutions

GREC2C3J- Combination

Epoch	YEAR	DOY	Sec of GPSweek	X-coordinates	Y-coordinates	Z coordinates	GPS rec clkoff	ZTD	ISB-GLO	ISB-GAL	ISB-BDS2	ISB-BDS3	ISB-J
1	2023	344	0.0000	-2713834.0349	5303935.3924	-2269513.8862	4.22257036	2.4152	4.815274	-1.087832	-11.242716	-13.285299	0.144028
2	2023	344	30.0000	-2713834.0962	5303935.6530	-2269513.7539	4.10381190	2.4509	4.777591	-1.098599	-11.747768	-13.057458	0.497471
3	2023	344	60.0000	-2713833.7695	5303935.3970	-2269513.6173	3.32058476	2.4550	4.643522	-1.129394	-12.246034	-13.055913	0.486037
4	2023	344	90.0000	-2713833.6109	5303935.1994	-2269513.5625	3.53679164	2.4718	4.651892	-1.215997	-12.448401	-13.157143	0.410967
5	2023	344	120.0000	-2713833.5476	5303935.0997	-2269513.5097	2.57528555	2.5016	4.595156	-1.211809	-12.557381	-13.175322	0.414741
6	2023	344	150.0000	-2713833.5667	5303935.0688	-2269513.5278	3.37640020	2.4945	4.649584	-1.183202	-12.645947	-13.182591	0.423367
7	2023	344	180.0000	-2713833.5776	5303935.1140	-2269513.5312	3.23832396	2.4636	4.679773	-1.154549	-12.683189	-13.107837	0.458845
8	2023	344	210.0000	-2713833.5609	5303935.1380	-2269513.5460	3.34021726	2.4437	4.653275	-1.174123	-12.795443	-13.116896	0.402039
9	2023	344	240.0000	-2713833.5556	5303935.1666	-2269513.5592	3.48796678	2.4336	4.640552	-1.202775	-12.872647	-13.145402	0.327419
10	2023	344	270.0000	-2713833.5247	5303935.1625	-2269513.5600	3.47868033	2.4334	4.646056	-1.202005	-12.900878	-13.181142	0.328036
11	2023	344	300.0000	-2713833.5276	5303935.1487	-2269513.5526	3.40871302	2.4341	4.627902	-1.227017	-12.889744	-13.204143	0.344981
12	2023	344	330.0000	-2713833.5321	5303935.1493	-2269513.5635	3.52387786	2.4330	4.683566	-1.193816	-12.848206	-13.181655	0.365718
13	2023	344	360.0000	-2713833.5382	5303935.1469	-2269513.5674	3.46291307	2.4343	4.693876	-1.185439	-12.854019	-13.158180	0.369135
14	2023	344	390.0000	-2713833.5363	5303935.1527	-2269513.5703	3.45773229	2.4346	4.703614	-1.182491	-12.880249	-13.143377	0.394208
15	2023	344	420.0000	-2713833.5166	5303935.1469	-2269513.5643	3.46753910	2.4368	4.677205	-1.195815	-12.908320	-13.146120	0.393350
16	2023	344	450.0000	-2713833.5008	5303935.1497	-2269513.5603	3.53430133	2.4394	4.681659	-1.195209	-12.908586	-13.145641	0.408117
17	2023	344	480.0000	-2713833.4963	5303935.1568	-2269513.5607	3.49023189	2.4402	4.666339	-1.210557	-12.929535	-13.140754	0.410309
18	2023	344	510.0000	-2713833.4916	5303935.1524	-2269513.5601	3.02324022	2.4440	4.666662	-1.208583	-12.954792	-13.148632	0.393308
19	2023	344	540.0000	-2713833.4942	5303935.1540	-2269513.5593	4.42356085	2.4462	4.667436	-1.214276	-12.978387	-13.161199	0.393541
20	2023	344	570.0000	-2713833.4927	5303935.1593	-2269513.5592	3.91637838	2.4469	4.670862	-1.220613	-12.991335	-13.160538	0.402280
21	2023	344	600.0000	-2713833.4785	5303935.1528	-2269513.5568	3.44875035	2.4498	4.679580	-1.201018	-12.992620	-13.157094	0.414267
22	2023	344	630.0000	-2713833.4640	5303935.1470	-2269513.5505	3.23443925	2.4540	4.682820	-1.203939	-13.005369	-13.159998	0.412049
23	2023	344	660.0000	-2713833.4572	5303935.1349	-2269513.5452	3.20454470	2.4569	4.686874	-1.203009	-13.010735	-13.161048	0.411980
24	2023	344	690.0000	-2713833.4530	5303935.1315	-2269513.5473	3.35926469	2.4587	4.693817	-1.205435	-13.012669	-13.169301	0.407412
25	2023	344	720.0000	-2713833.4461	5303935.1304	-2269513.5476	2.75918639	2.4607	4.684635	-1.212339	-13.038025	-13.182026	0.397027
26	2023	344	750.0000	-2713833.4447	5303935.1293	-2269513.5460	3.33552251	2.4609	4.683613	-1.212719	-13.048265	-13.172319	0.390097
27	2023	344	780.0000	-2713833.4417	5303935.1271	-2269513.5456	2.69888222	2.4621	4.687208	-1.210413	-13.037740	-13.162449	0.381868
28	2023	344	810.0000	-2713833.4379	5303935.1235	-2269513.5446	3.08515719	2.4637	4.687561	-1.216446	-13.031272	-13.164061	0.377765
29	2023	344	840.0000	-2713833.4351	5303935.1210	-2269513.5424	2.73305192	2.4653	4.684935	-1.213310	-13.023514	-13.169446	0.367375
30	2023	344	870.0000	-2713833.4331	5303935.1199	-2269513.5409	3.19394905	2.4668	4.683724	-1.215409	-13.024438	-13.170830	0.361235
31	2023	344	900.0000	-2713833.4286	5303935.1203	-2269513.5399	2.62776773	2.4679	4.687429	-1.213271	-13.040468	-13.172969	0.353694
32	2023	344	930.0000	-2713833.4270	5303935.1195	-2269513.5402	3.05852285	2.4680	4.694492	-1.215382	-13.049441	-13.174525	0.349365
33	2023	344	960.0000	-2713833.4265	5303935.1209	-2269513.5417	3.16124117	2.4674	4.701645	-1.207598	-13.052328	-13.168738	0.356316
34	2023	344	990.0000	-2713833.4269	5303935.1256	-2269513.5427	2.85370748	2.4663	4.707010	-1.209663	-13.057895	-13.174355	0.364877
35	2023	344	1020.0000	-2713833.4242	5303935.1262	-2269513.5423	3.11555293	2.4656	4.717857	-1.204011	-13.057822	-13.170132	0.374460
36	2023	344	1050.0000	-2713833.4256	5303935.1256	-2269513.5422	2.70197022	2.4652	4.709686	-1.197778	-13.057535	-13.163106	0.374229
37	2023	344	1080.0000	-2713833.4231	5303935.1244	-2269513.5416	3.02617108	2.4652	4.708657	-1.196011	-13.034261	-13.157021	0.378149
38	2023	344	1110.0000	-2713833.4221	5303935.1253	-2269513.5409	2.92183185	2.4653	4.716732	-1.191764	-13.017409	-13.148846	0.376819
39	2023	344	1140.0000	-2713833.4203	5303935.1262	-2269513.5405	3.11465608	2.4650	4.715558	-1.195540	-13.018867	-13.147922	0.374974
40	2023	344	1170.0000	-2713833.4207	5303935.1280	-2269513.5414	2.54678290	2.4644	4.721606	-1.196636	-13.010788	-13.142909	0.382306
41	2023	344	1200.0000	-2713833.4209	5303935.1291	-2269513.5417	3.16335745	2.4642	4.724549	-1.195210	-12.998325	-13.139830	0.392739
42	2023	344	1230.0000	-2713833.4216	5303935.1307	-2269513.5416	2.75029572	2.4636	4.721027	-1.198911	-13.003172	-13.148906	0.384215
43	2023	344	1260.0000	-2713833.4237	5303935.1296	-2269513.5419	2.74171298	2.4636	4.711019	-1.200184	-12.985881	-13.161719	0.385900

Figure 16. The output file of the KARR station, which was obtained from the GREC2C3J combination

5.2. PPP Performance Analysis

The ground truth coordinates of the station and the tropospheric delay products provided by IGS can be imported into the software with the Outputs>Analysis submenu to assess the performance of PPP. By entering the reference data shown in Figure 17, the Calculate button is pressed to obtain the North, East, Up, 3D, and ZTD RMS values depending on the convergence criterion. In addition, the convergence time, which is the primary disadvantage of PPP, is calculated as a minute.

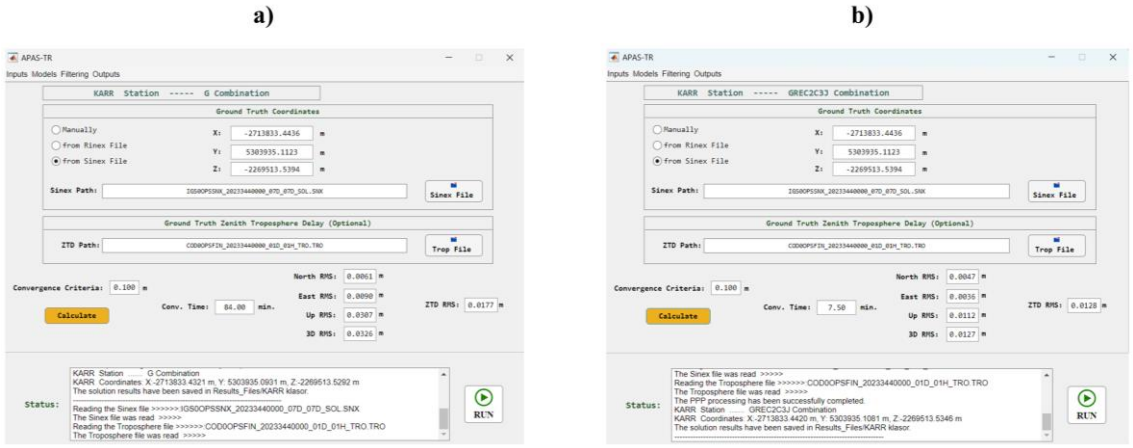

Figure 17. PPP performance and accuracy analysis for different GNSS configurations a) GPS-only combination b) GREC2C3J multi-GNSS combination

Figure 17 displays the results of single-GPS and multi-GNSS (GREC2C3J) PPP solutions. Multi-GNSS findings show substantial improvements in convergence time and accuracy criteria compared with single-GNSS results. The convergence time was less than 10 minutes due to the significant number of satellites and good satellite geometry. Multi-GNSS PPP produced an RMS value of approximately 1.1 cm for the vertical component, while the horizontal positioning accuracy was less than 1 cm. Also, the tropospheric estimate accuracy of about 1.3 cm is noteworthy for atmospheric research.

5.3. Plotting

The plotting tools of the software are available using the Outputs>Plotting submenu. When finished with the PPP process and analysis, many visualizations can be used for interpretation and evaluation. The plotting tools are depicted in Figure 18. Before moving on to the residual

analysis, the drawing outputs of the multi-GNSS results of the KARR station can be listed as follows.

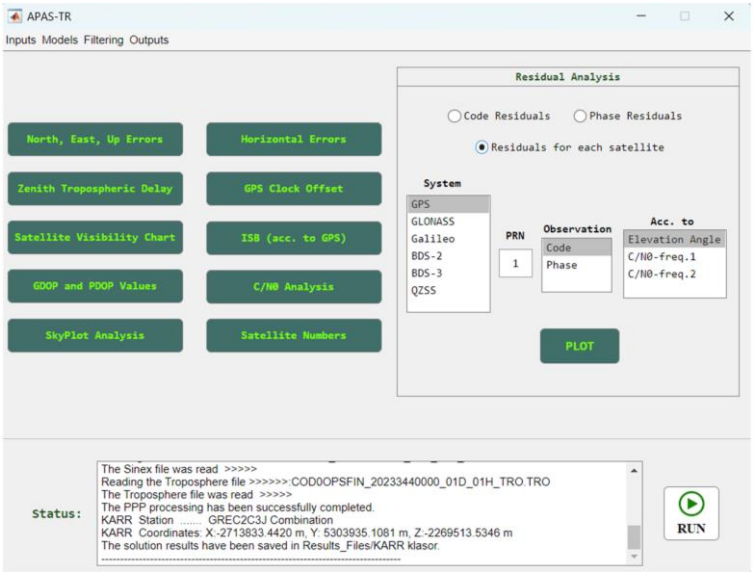

Figure 18. Plotting tools of the software

5.3.1. North, East, and Up Errors

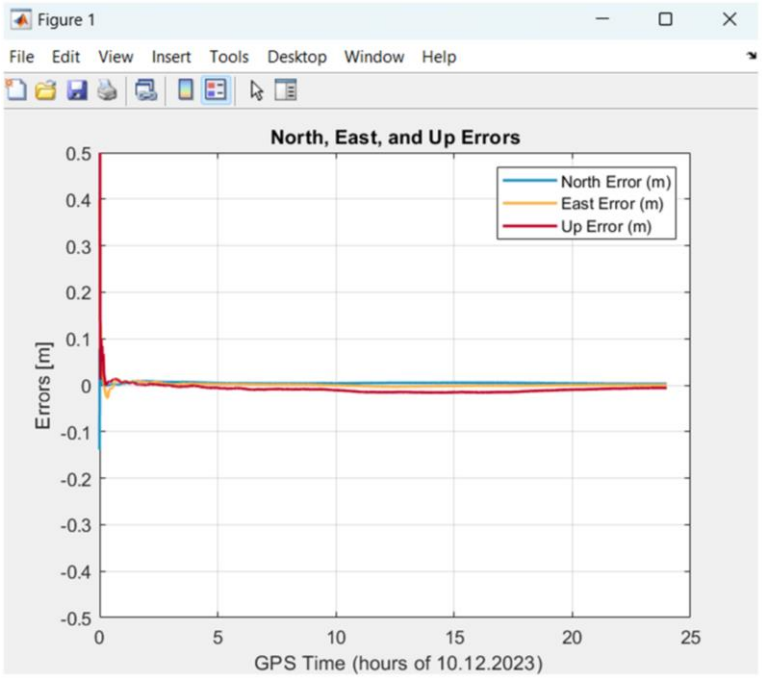

5.3.2. Horizontal Errors

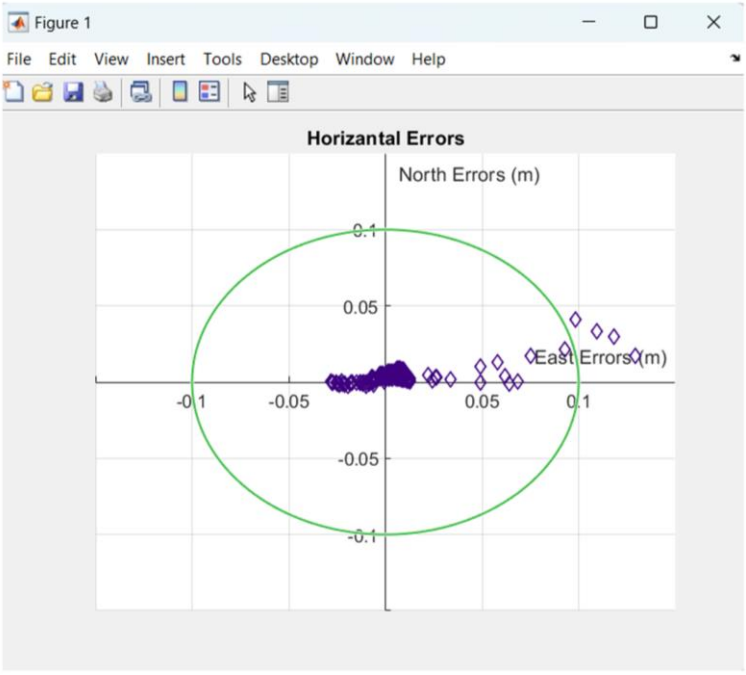

5.3.3. Zenith Tropospheric Delay

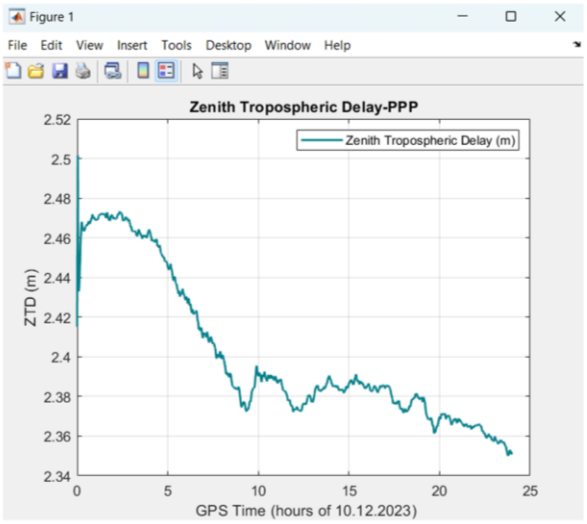

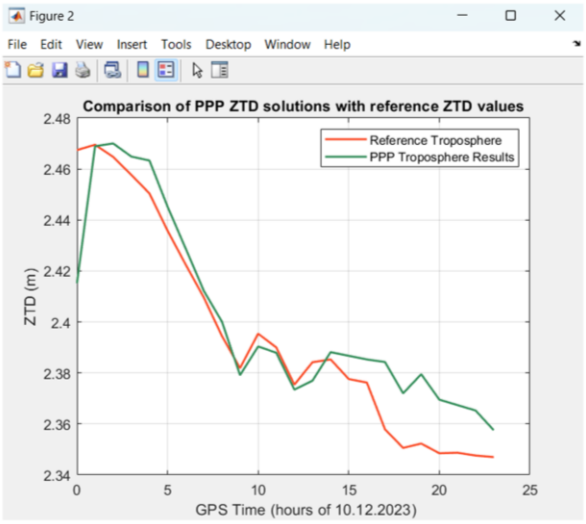

5.3.4. GPS Receiver Clock Offset

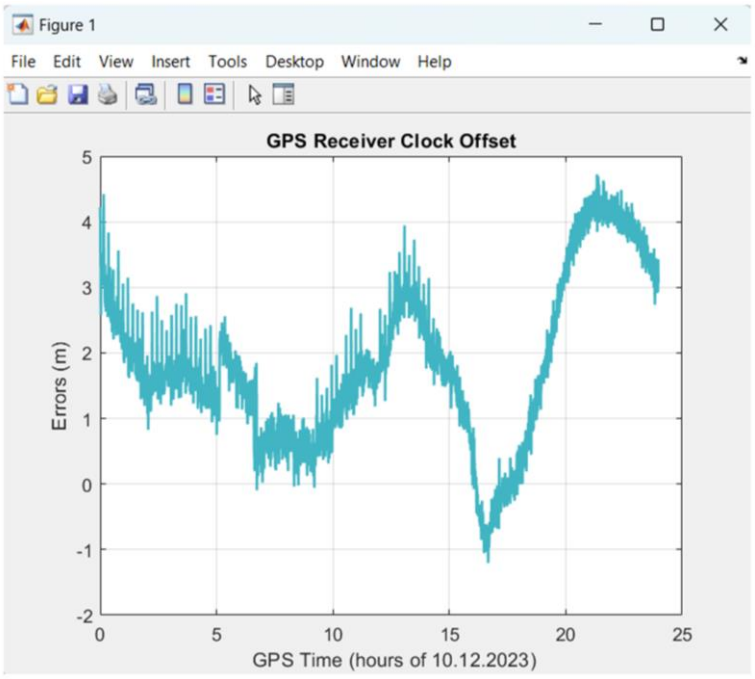

5.3.5. Satellite Visibility Chart

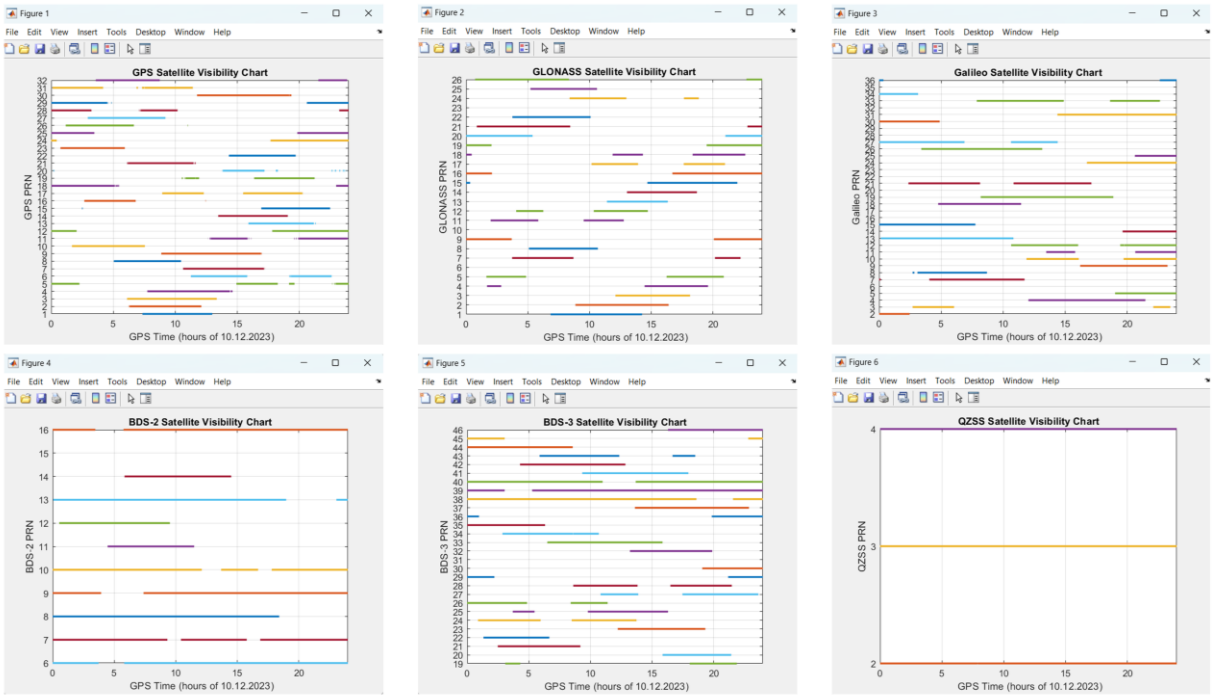

5.3.6. ISB (acc. to GPS)

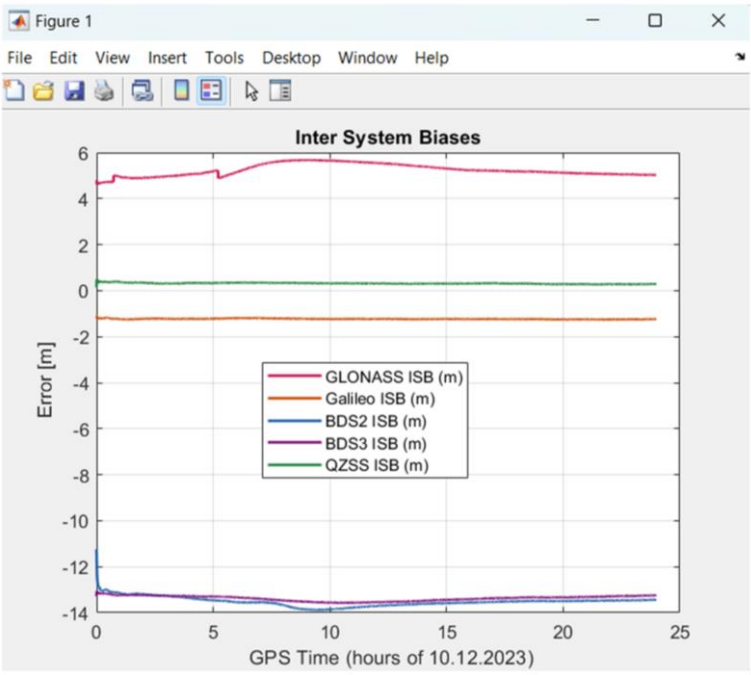

5.3.7. GDOP and PDOP Values

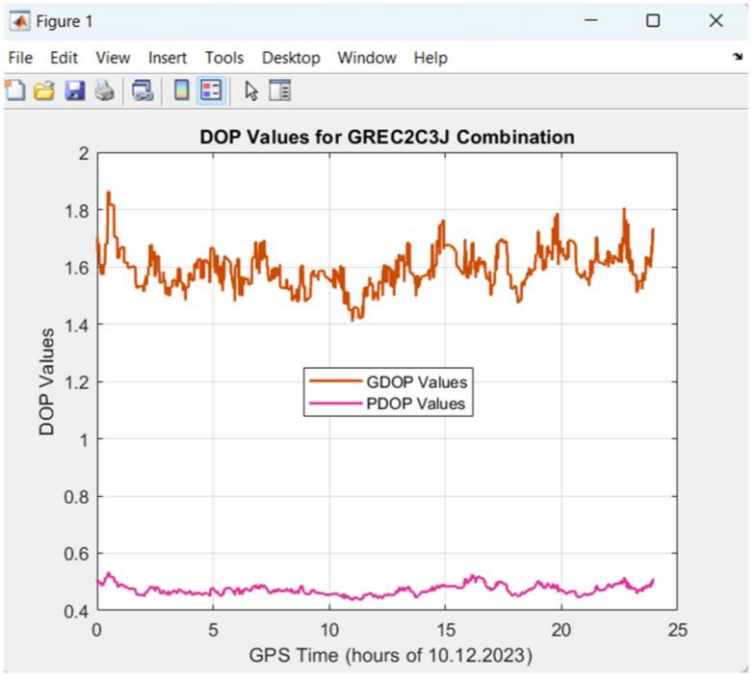

5.3.8. C/N0 Analysis

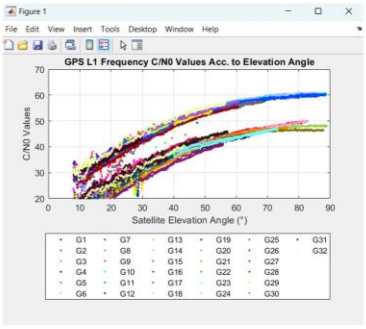

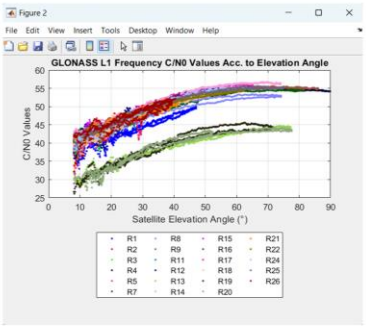

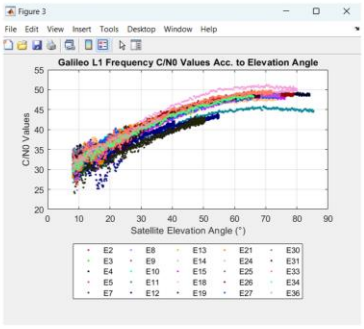

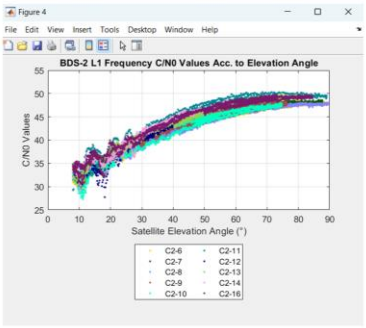

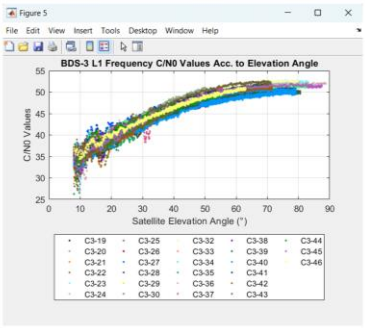

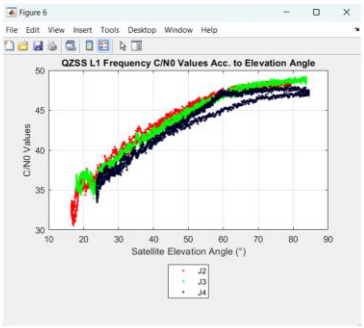

5.3.9. SkyPlot Analysis

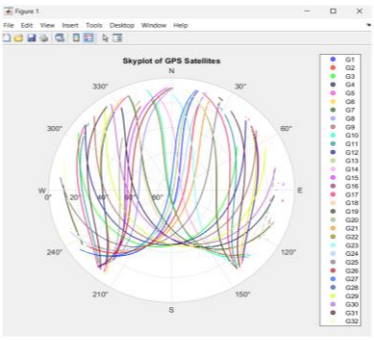

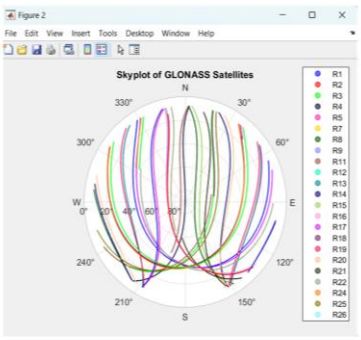

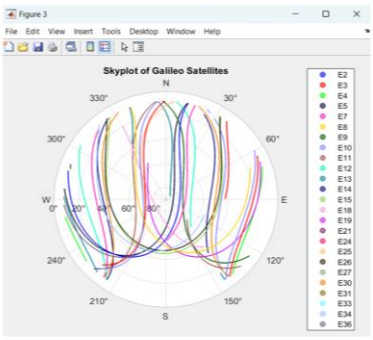

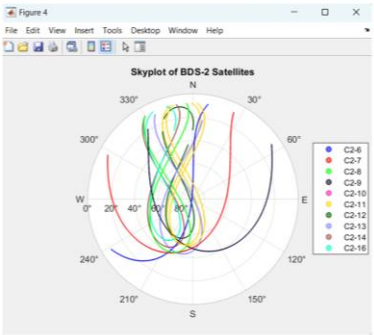

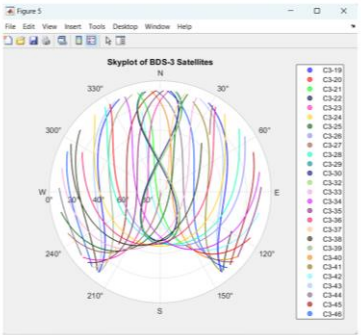

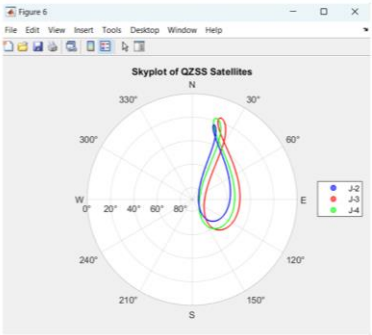

5.3.10. Satellite Numbers

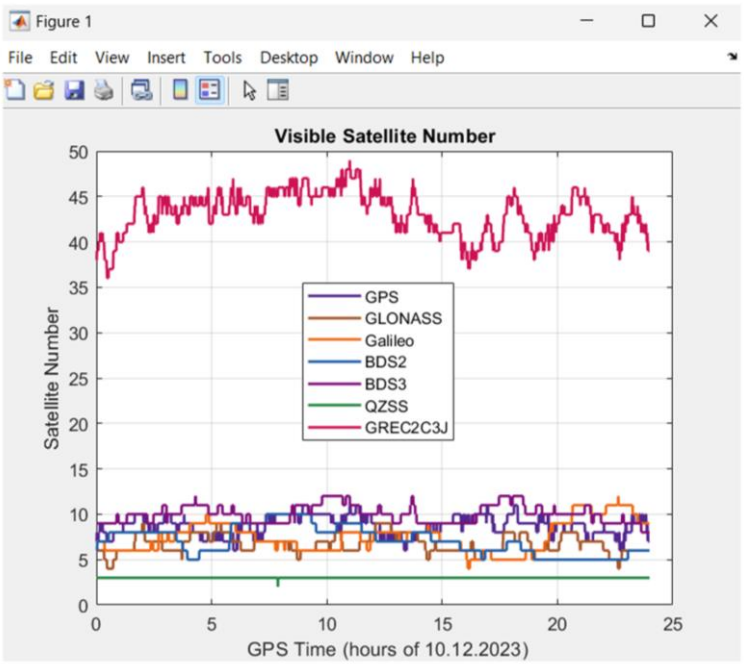

5.3.11. Residual Analysis (Code Residuals)

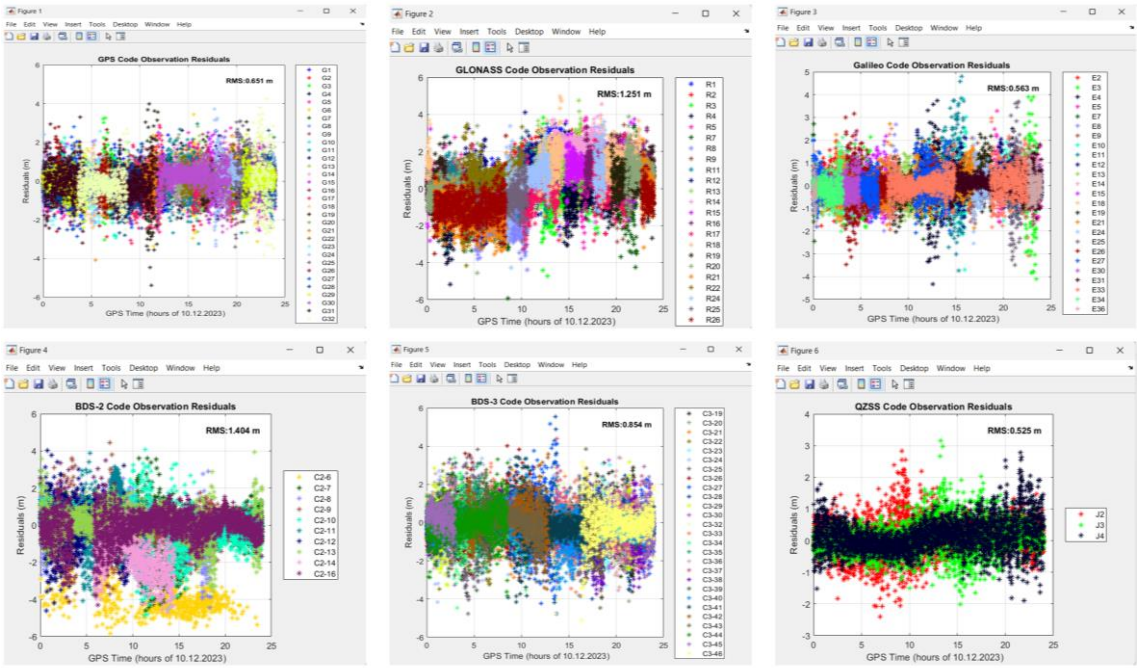

5.3.12. Residual Analysis (Phase Residuals)

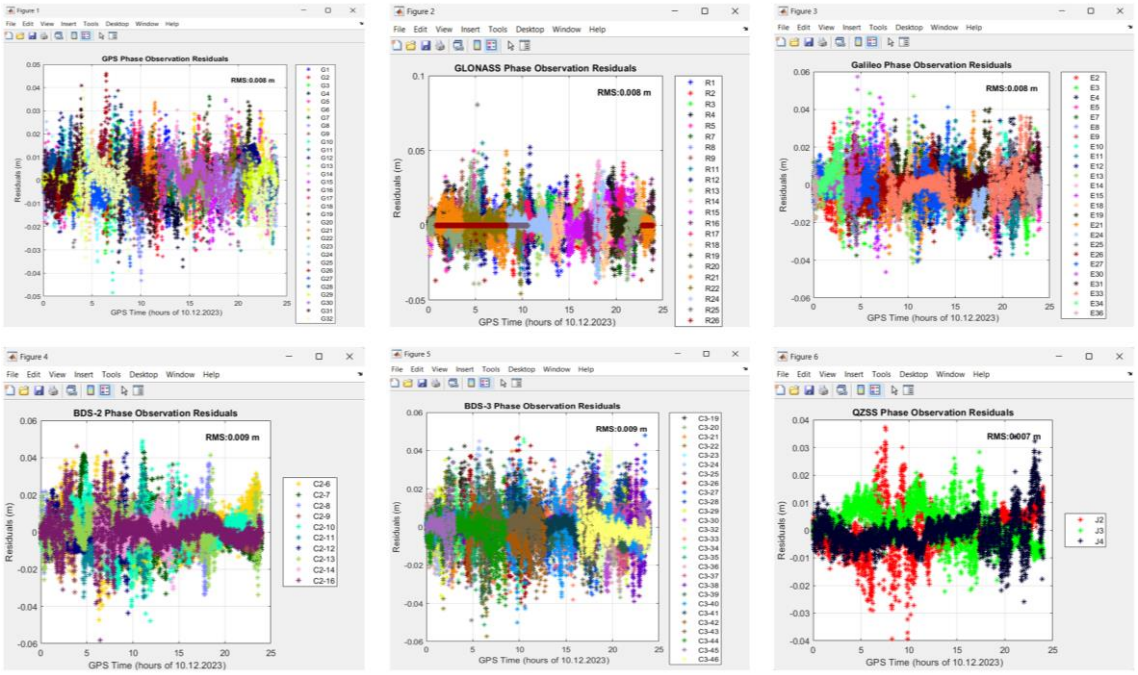

5.3.13. Residual Analysis (Code and Phase Residuals for each satellite)

A residual analysis can be carried out for each satellite used in the solution. The residuals of the code and phase observations of the GPS PRN 01 satellite selected as an example can be plotted with respect to different criteria (elevation angle, C/N0 value for the first and the second frequency) as follows.

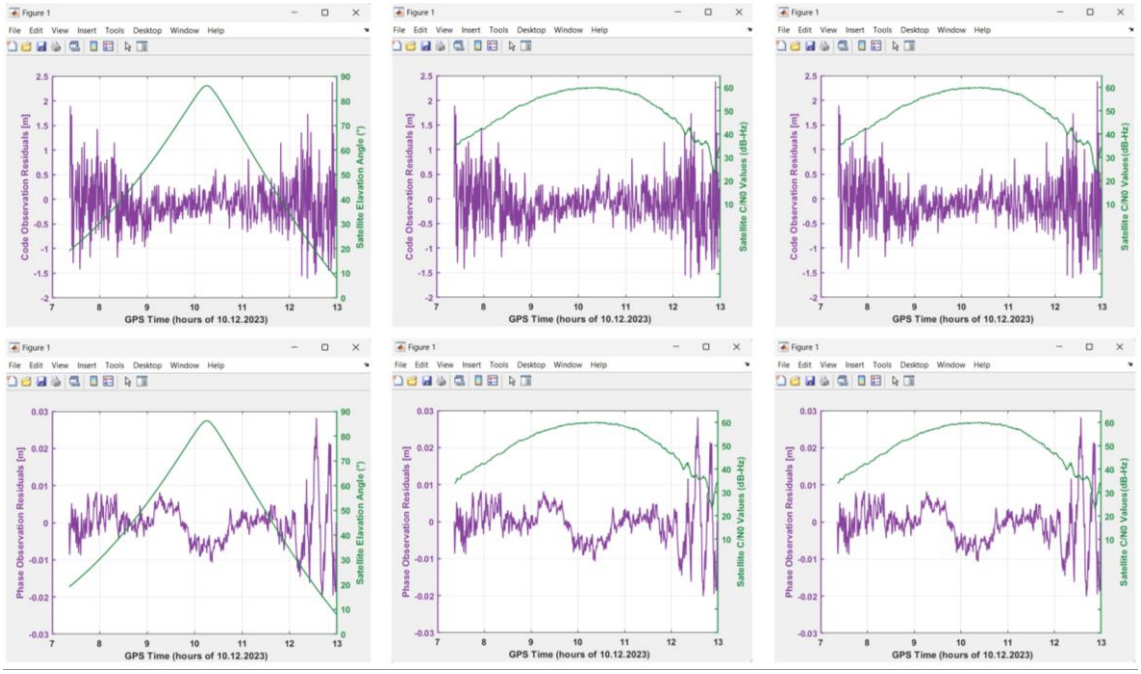

6. PPP Processing using APAS_TR_without_Interface MATLAB Code

The software package also offers the ability to implement PPP without an interface. Indeed, the PPP evaluation procedure can be performed manually using **APAS_TR_without_Interface.m.** In the code, the names of the input files must be entered correctly in the relevant places. Subsequently, any changes that are made in the interface can also be made here. The code is set for the PPP solution of the KARR station. As a result, when this code is executed, it will give the same results as those obtained from the interface.

7. References

Askne J, Nordius H (1987) Estimation of tropospheric delay for microwaves from surface weather data. Radio Sci 22(3):379–386. https://doi.org/10.1029/RS022i003p00379

Blewitt G (1990) An Automatic Editing Algorithm for GPS data. Geophys Res Lett 17(3):199–202. https://doi.org/10.1029/GL017i003p00199

Boehm J, Werl B, Schuh H (2006) Troposphere mapping functions for GPS and very long baseline interferometry from European Centre for Medium-Range Weather Forecasts operational analysis data. J Geophys Res Solid Earth 111(B2):1–9. https://doi.org/10.1029/2005JB003629

Böhm J, Möller G, Schindelegger M, Pain G, Weber R (2015) Development of an improved empirical model for slant delays in the troposphere (GPT2w). GPS Solut 19(3):433–441. https://doi.org/10.1007/s10291-014-0403-7

Cai C, Liu Z, Xia P, Dai W (2013) Cycle slip detection and repair for undifferenced GPS observations under high ionospheric activity. GPS Solut 17(2):247–260. https://doi.org/10.1007/s10291-012-0275-7

Guo F, Zhang X (2014) Real-time clock jump compensation for precise point positioning. GPS Solut 18(1):41–50. https://doi.org/10.1007/s10291-012-0307-3

Kouba J (2008) Implementation and testing of the gridded Vienna Mapping Function 1 (VMF1). J Geod 82(4–5):193–205. https://doi.org/10.1007/s00190-007-0170-0

Landskron D, Böhm J (2018) VMF3/GPT3: refined discrete and empirical troposphere mapping functions. J Geod 92(4):349–360. https://doi.org/10.1007/s00190-017-1066-2

Leandro R, Santos M, Langley RB (2006) UNB neutral atmosphere models: Development and performance. Proc Inst Navig Natl Tech Meet 2:564–573

Luo X, Du J, Lou Y, Gu S, Yue X, Liu J, Chen B (2022) A Method to Mitigate the Effects of Strong Geomagnetic Storm on GNSS Precise Point Positioning. Sp Weather 20(1):1–13. https://doi.org/10.1029/2021SW002908

Saastamoinen J (1972) Atmospheric Correction for the Troposphere and Stratosphere in Radio Ranging Satellites. Use Artif Satell Geod 15(4):247–251. https://doi.org/10.1029/GM015p0247